Journal of Imaging Science and Technology® 51(5): 456–460, 2007.

Top Contact Organic Thin Film Transistors with Ink Jet Printed Metal Electrodes

Kuo-Tong Lin, Chia-Hsun Chen, Ming-Huan Yang, Yuh-Zheng Lee and Kevin Cheng
Display Technology Center, Industrial Technology Research Institute Hsinchu, Taiwan 310, Republic of China
E-mail: BillyLin@itri.org.tw

Abstract. *Ink jet printing conductive metal nanopastes have been studied in research on printed circuit boards and passive components. This technique provides a manufacturing method that can replace more expensive processes, such as lithography or metal evaporation. In this paper, we demonstrated a printed silver top-contact source-drain electrodes on bottom-gate organic thin film transistors (OTFTs). The soluble conjugated polymer, regioregular poly(3-hexylthiophene) (RR-P3HT), was used as the active channel material. To increase electric transport efficiency by tuning the surface hydrophibic characteristics, a buffer layer, V_2O_5, between organic semiconductor and printed electrodes, was introduced to resolve the incompatibility of these two layers. The results indicated the printed Ag on V_2O_5 film is hydrophilic (contact angle ~10°), different with that on P3HT only (hydrophibic, contact angle about 65°). High hydrophilic surface of V_2O_5 led to self-aligning behavior of patterned Ag nanopastes and is helpful to get a flat film. This study also compares the characteristics of OTFTs to traditionally evaporated electrodes and to ink jet printed source-drain electrodes, in order to analyze the mechanism action of the buffer layer and its related process differences. © 2007 Society for Imaging Science and Technology.*
[DOI: 10.2352/J.ImagingSci.Technol.(2007)51:5(456)]

INTRODUCTION

In recent years, a trend in developing new electronic devices is to minimize the element size and to increase the density of devices, which is a solution to reducing cost and simplifying processing.[1] The major cost of fabricating an electronic device comes from the processing procedures rather than from the raw materials. Traditional photolithography and the high vacuum process can produce devices that scale down to several micrometers, but the infrastructures are expensive. Low cost process technologies for fabricating electronic devices include screen printing,[2,3] micromolding in capillaries,[4] soft lithographic stamping,[5] and ink jet printing.[6] The reduction of processing procedures through direct deposition of a material could reduce the cost and complexity of the fabrication process further. Ink jet printing is a potential alternative to the existing deposition approaches. As a maskless process, it can reduce the cost of physical molding and chemical waste of material. Moreover, ink jet printing technology is much easier extended to process on a large area substrate than are other processes.

Overarching inks can be used for the process of ink jet printing. These inks comprise inorganic and organic electronic materials and are expected to form wiring, electrodes, and many other kinds of components of an electric device. The application of ink jet printed electronic devices includes thin film transistors (TFTs), radio frequency identification (RFID) circuits, organic light-emitting diodes (OLED), and printed circuit boards (PCBs).[7] Among various inks used in the past few years, conducting inks have been newly developed for forming the electrodes of the devices. Poly(ethylene dioxythiophene) (PEDOT) is a good candidate for forming ink jet printed electrodes, but the conductivity is several orders lower than that of metals. The conductivity of the metal nanopastes is three to four orders higher than that of PEDOT. After low temperature sintering (150°C), the nanoparticles form aggregates, and film thickness can be controlled by tuning the drop size and the solid content of the inks. The fabrication processes for flexible display devices require low processing temperatures, however.

Burgi et al.[8] discussed the influence of the work function for the metal on the device performance with poly(3–hexylthiophene) (PHT) as an active layer. The source/drain metal electrode is chosen to be Cr/Au, Ag, or Au only. Other metals form Schottky barriers at the interface so that the resistance is high and the current is blocked therein.

This study explored the effects of various printing conditions with a Dimatix SE-128 piezoelectric printhead on the quality of the printed film, and we discuss the influence of the thin transition metal buffer layer on TFT device performance. Using a transition metal oxide as the hole injection layer is an effective way to improve the characteristics of organic thin film transistors (OTFTs).[9] At the same time, the contact angle of the nanopaste on the transition metal oxide is smaller than that on P3HT; thus, the printing quality of the metal line is better. Furthermore, the thickness of this buffer layer is so thin that device performance is not significantly influenced.

TOP CONTACT–BOTTOM GATE OTFT STRUCTURE AND PROCESSES

The structure of the organic thin film transistor with ink jet printed silver electrodes is shown in Figure 1. The bottom gate with heavily doped Si is selected, and SiO_2 with thickness of 300 nm is used as the gate dielectric. The Si/SiO_2 substrate was cleaned sequentially with acetone and isopro-

Received Jan. 17, 2007; accepted for publication Jun. 20, 2007.
1062-3701/2007/51(5)/456/5/$20.00.

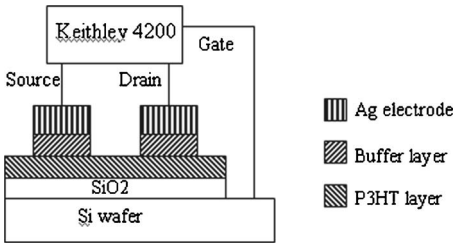

Figure 1. The structure of the polymer thin film transistor device (PTFT) with a silver top electrode.

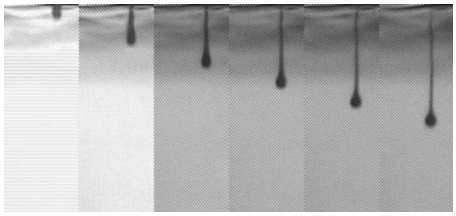

Figure 2. Observation of the break-off behavior of the printed drop beneath an arbitrary nozzle.

Table I. Contact angles for silver nanopaste on the P3HT and V_2O_5.

Substrate	Contact Angle
P3HT	65°
V_2O_5	<10°

panol in an ultrasonic bath. After 150 W, 450 mtorr, and 5 min, oxygen plasma treatment, a monolayer of OTS was self-assembled onto the SiO_2 layer by dipping the substrate (with SiO_2 layer) into the 60°C OTS dilute toluene solution for 20 min. Then, regioregular poly(3-hexylthiophene) (P3HT) (purchased from Rieke) was used as the organic active layer. P3HT dissolved in xylene (0.5 wt. %) was spin coated on the substrate and baked at 90°C for 90 mins. The thickness of this P3HT film was about 50 nm. The transition metal buffer layer comprised of dielectric material, vanadium oxide (V_2O_5),was then thermally evaporated by shadow mask on the P3HT; its thickness was 3 nm. The shape of V_2O_5 layer is defined by a metal mask, and Ag is ink jet printed approximately within the area of V_2O_5. The printing position need not to be correctly defined, since the surface energy behavior self-aligns this Ag ink on the low contact angle surface, i.e., V_2O_5. To compare the performance of this device with ink jet printed silver nanopaste top electrodes, we made a device with evaporated silver film top electrodes.

The ink jet printing platform, developed by the Display Technology Center (DTC) in the Industrial Technology Research Institutes (ITRI), equipped with Dimatix SE-128 piezoelectric printhead, was used to discharge the silver nanoparticle inks (AG-IJ-G-100-S1), purchased from Cabot. The low resistivity patterned silver film was obtained after postbaking at 150°C for 30 min in a glove box to sinter the

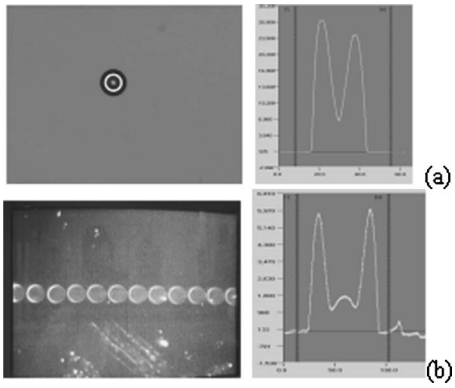

Figure 3. Profiles of the sintered silver nanopaste dot formed by ink jet printing on the different substrates: (a) P3HT and (b) V_2O_5.

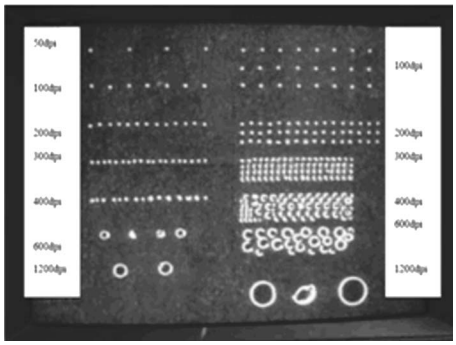

Figure 4. Morphology of the sintered silver nanopaste dot formed by ink jet printing on the P3HT substrate with different drop densities.

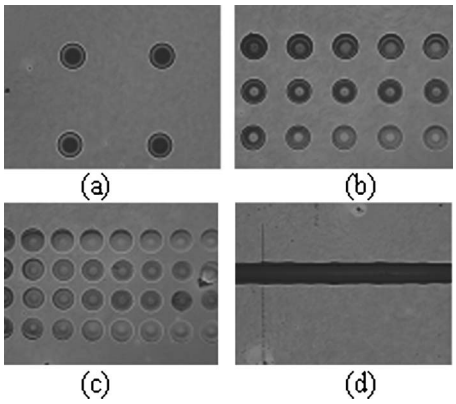

Figure 5. Morphology of the sintered silver nanopaste dot formed by ink jet printing on the V_2O_5/P3HT substrate with different drop densities: (a) 100 dpi, (b) 200 dpi, (c) 300 dpi, and (d) 400 dpi.

predeposited precursor material. The thickness of the metal layer was 200 nm. In contrast, the pressure of the chamber was maintained at about 5×10^{-6} torr during evaporation of silver electrodes. Finally, measurements of V_D versus I_D and V_G versus I_D for devices were conducted using a Keithley 4200 semiconductor parameter analyzer.

The field effect mobility μ was calculated in the saturation regions from the following equation:

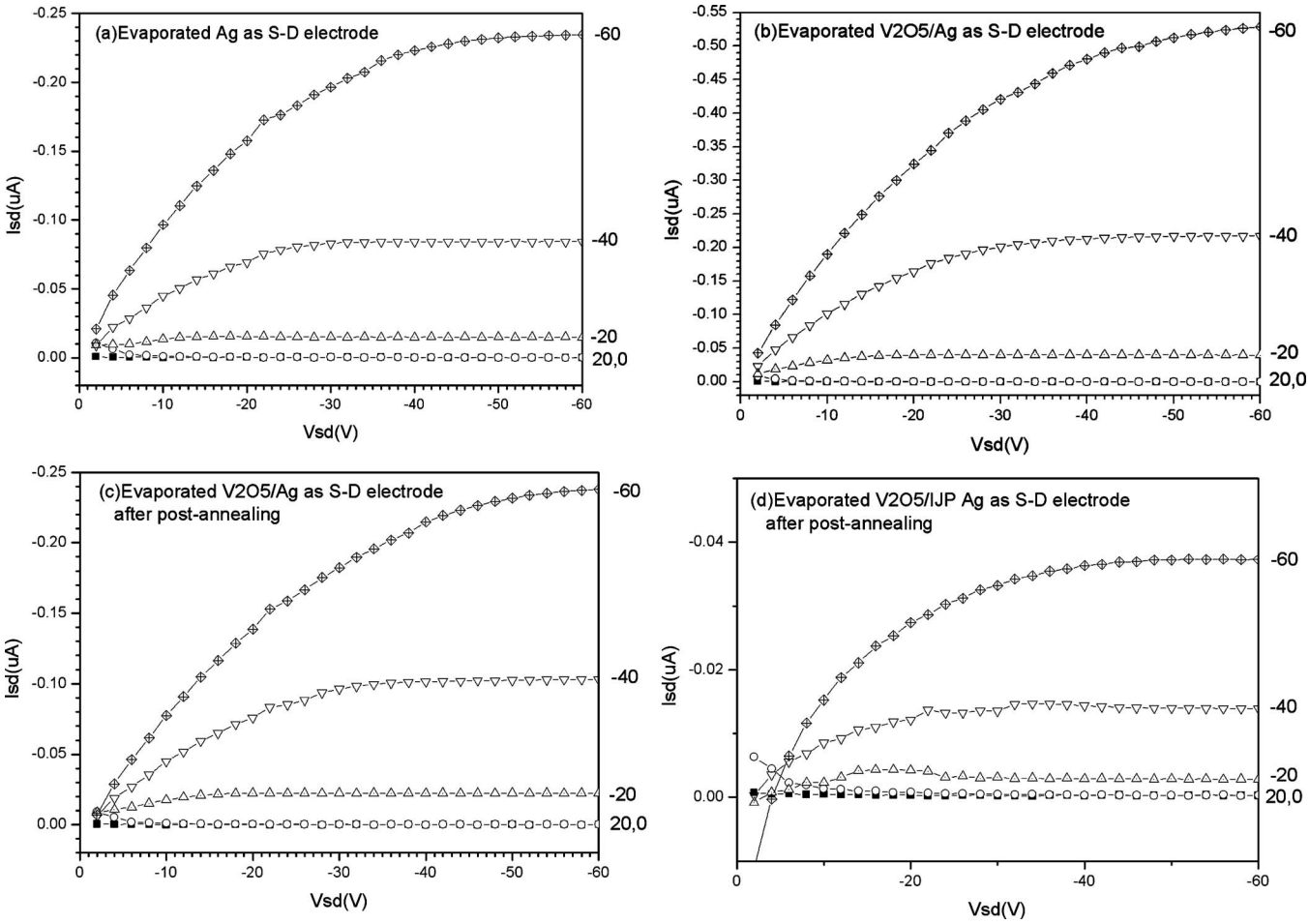

Figure 6. I_d-V_{ds} characteristics of the PTFT, wherein the source-drain electrodes are: (a) evaporated Ag, (b) evaporated V_2O_5/Ag, (c) evaporated V_2O_5/Ag with postannealing, and (d) evaporated V_2O_5/IJP Ag with postannealing.

$$I_{DS} = (WC_i/2L)\mu(V_G - V_T)^2, \quad (1)$$

where W is the channel width, L is the channel length, C_i is the capacitance per unit area of the insulator, and V_T is the threshold voltage.

RESULTS AND DISCUSSION

Stability of the Ink Jet Printed Ink

This study improved the jetting behavior of piezoelectric print heads by controlling three parameters, i.e., pulse waveform, pulse frequency, and driving voltage. Suitable range of waveform modulation and pulse frequency are defined corresponding to given driving voltages for appropriate ink discharging. The jetting behavior can be observed by using a strobe image capturing system integrated in the printing platform. The break-off behavior of the jettable silver nanoparticles ink was captured within 60 μs and shown in Figure 2. The velocity of the jetted drop was about 6.4 m/s and stable. With a stand-off of 1 mm, we successfully modulated the ink jet printing parameters of Dimatix SE-128 for silver nanoparticles of ink, and obtained uniform and continuous silver paste lines.

Table II. Electrical characteristics of the various PTFTs.

S-D Electrodes	Mobility (cm^2/V.s)	Threshold Voltage (V)	On/Off Ratio
Evaporate Au	3.48×10^{-3}	–9.49	14268
Evaporate Ag	1.88×10^{-3}	–11.17	629
Evaporate V_2O_5/Ag	2.23×10^{-3}	–10.63	1398
Evaporate V_2O_5/Ag (with postannealing)	1.19×10^{-3}	–9.95	3107
Evaporate V_2O_5/IJP Ag (with postannealing)	2.98×10^{-4}	–15.27	138

Morphology of the Ink Jet Printed Nanopaste

The contact angles of the silver nanopaste between the P3HT film and the V_2O_5 buffer film are shown in Table I. The contact angle on P3HT film is 65°, which is larger than that on the V_2O_5 film. The morphology of printed nanopaste is related to the contact angle on the surface. The morphologies of the nanopaste on these two substrates are shown in Figure 3. As the nanopaste ink jet printed on the P3HT film was postannealed, the dot diameter shrunk to about 30 μm

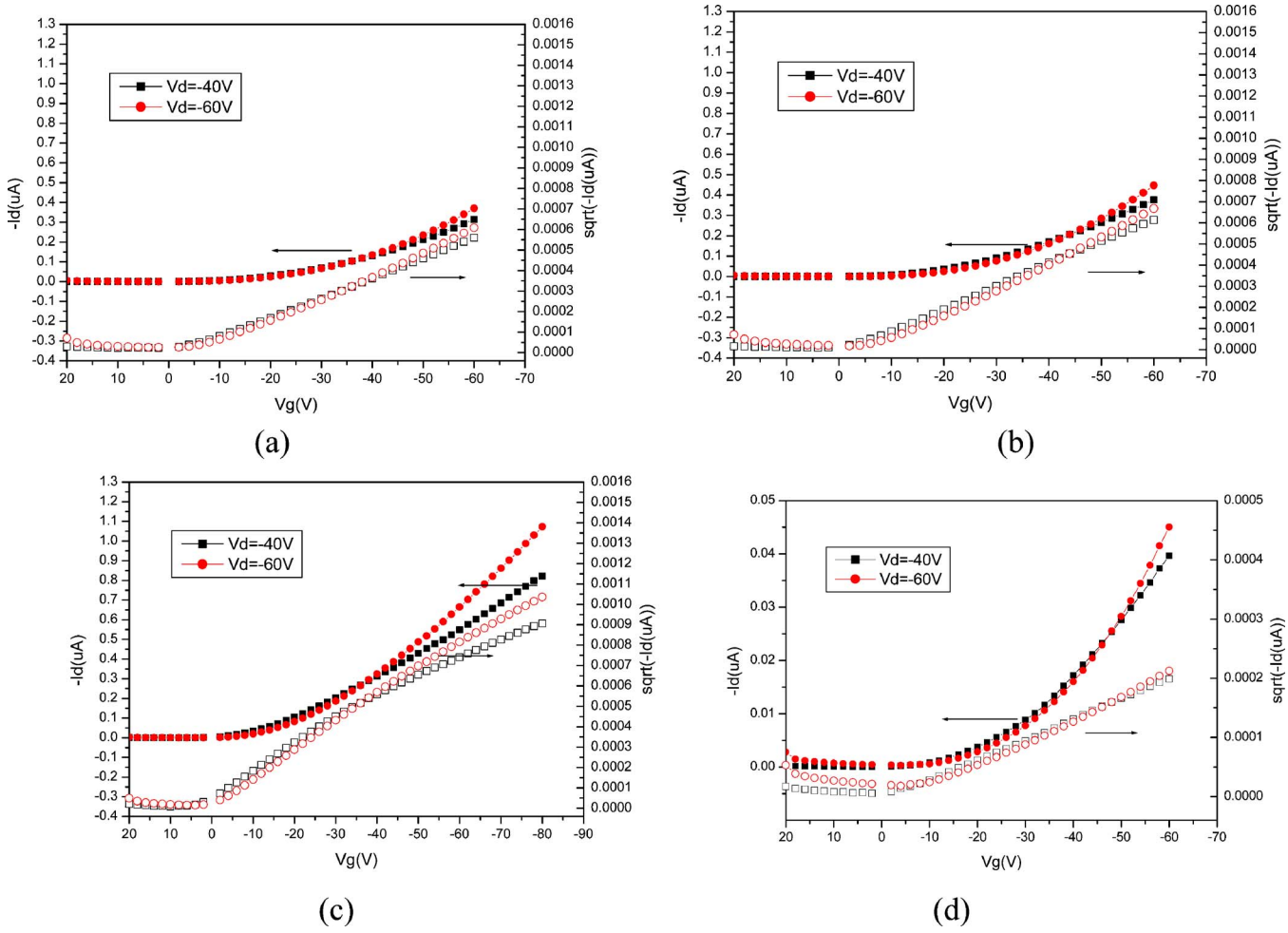

Figure 7. I_d-V_{gs} characteristics of the PTFT, wherein the source-drain electrodes are: (a) evaporated Ag, (b) evaporated V_2O_5/Ag, (c) evaporated V_2O_5/Ag with postannealing, and (d) evaporated V_2O_5/IJP Ag with postannealing.

and formed a coffee-ring structure. The thickness of the ring edge was ~2.5 μm. The drop morphology on P3HT alone was so rough that it was difficult to form a flat film and pattern uniform metal electrodes. On the other hand, it was a good choice to print nanopaste on V_2O_5/P3HT film. The dot size was 73 μm and did not shrink. A coffee ring still formed, but the morphology of the dot was flatter, and it was easier to construct lines and patterns of metal electrodes. The ring thickness was ~0.5 μm. In addition, the more hydrophilic surface of V_2O_5 led to self-aligning behavior of patterned Ag nanopastes. After sintering the patterned Ag nanopaste at 150°C for 30 min, the resultant resistivity of the ink jet printed electrode was about 3×10^{-8} Ω m, which was two to three times that for the normal bulk silver.

Currently, no OTFT-related article has reported how to ink jet print Ag ink onto the semiconductor layer and discussed the resulting interface. All of the previously reported devices were bottom-contact devices, and Ag ink was printed onto the dielectric layer. However, the contact angle of Ag ink to hydrophilic dielectric layer was small, and the printed pattern was easy to fix in position. On the other hand, the contact angle of Ag ink to the hydrophibic organic semiconductor was large, which makes the printed ink deposits shrink relative to each other, and it is accordingly hard to form a uniform film, as shown in Figure 4. In this article an approach is proposed to improve the morphology of the electrode ink on the semiconductor by inserting an inorganic buffer layer. The morphology of the nanopaste on V_2O_5/P3HT film is shown in Figure 5. As the printing density increased to 400 dpi, the drops began to aggregate and formed uniform lines or patterns. The best printing density was found to be ~400 dpi, with the width of the line ~62 μm. Further increase in the printing density led to thicker and wider conductive Ag lines. If we discharged denser inks, it would be harder to control the morphology because more ink would lead to unstable boundaries of the Ag lines.

DEVICE PERFORMANCE

The source-drain (S-D) electrodes are bilayer electrodes formed on the organic active layer. The channel width and length of each device were 2000 μm and 140 μm, respectively. The device performance is stable, on the basis of the averaged results obtained with three devices. Basically, no obvious difference was found in device performance between evaporated silver and bilayer V_2O_5/Ag electrodes. The

results are shown in Figures 6(a) and 6(b). The device with the Ag S-D electrode had an on-off ratio (I_{on}/I_{off}) and mobility similar to the device with V_2O_5/Ag S-D electrode. The on-off ratio was near 10^3, and the mobility was $\sim 10^{-3}$ cm^2/V s. However, the current of the V_2O_5/Ag S-D electrode was about twofold larger than that of the device with Ag S-D electrode, indicating better hole injection after inserting the V_2O_5, which can also be a hole injection layer as well as providing surface energy modification. In the case of ink jet printed silver electrode, the patterned modification of the V_2O_5 buffer layer was necessary for the correct definition of the S-D boundary. The Ag nanopaste ink was self-aligned onto the patterned S-D V_2O_5 buffer layer and did not deposit onto the P3HT due to the differences in contact angle, i.e., the surface energy. The device performance after postannealing is shown in Figs. 6(c) and 6(d). We observed that there is no decrease in the performance of the device with evaporated S-D electrodes after postannealing at 150°C for 30 min. The performance of the device with ink jet printed Ag electrode was not as good. The mobility and current dropped one order of magnitude, which may be due to the conductivity decrease of the ink jet printed Ag electrode and organic residuals from the nanopastes being present at the metal/semiconductor interface. These results are summarized in Table II. It is worth noting that the choice of S-D electrode and interface engineering are important. The I_d-V_{gs} characteristics of these four devices are shown in Fig. 7 for comparison. There are some leakage currents in our newly developed device, which we will discuss and try to improve in the future.

CONCLUSION

In this paper, we successfully demonstrated a top contact–bottom gate OTFT device fabricated by ink jet printing silver nanopaste electrode, along with thermally evaporation and spin coating. By modulating the ink jet printing parameters, a well-sintered silver electrode was formed to fabricate a TFT device with a channel width of $\sim$2000 μm and channel length of $\sim$140 μm. The morphology of the nanopaste drop on the P3HT was rough, and it was hard to form flat lines and patterns of the metal electrodes; thus, we introduced a thin transition metal oxide as the buffer layer. The more hydrophilic surface of V_2O_5 led to self-aligning behavior of patterned Ag nanopaste, and a continuous conductive line could be formed. The current of the V_2O_5/Ag S-D electrode was about twofold larger than that of a device with an evaporated Ag S-D electrode, indicating better hole injection after inserting the V_2O_5, which can also be a hole injection layer, as well as providing surface energy modification. The device performance of the ink jet printed Ag electrode was inferior to that of the evaporated one after annealing. The mobility and current dropped one order of magnitude, which may be due to the conductivity decrease of the ink jet printed Ag electrode post annealing and the organic residuals from the nanopaste present in the metal/semiconductor interface. In the future, we expect to improve the interface between the S-D electrodes and the semiconductor layer of the printed OTFT device to achieve comparable performance to an evaporated or spin-coated counterpart.

REFERENCES

[1] P. Calvert, Chem. Mater. **13**, 3299 (2001).
[2] C. D. Sheraw, L. Zhou, J. R. Huang, D. J. Gundlach, T. N. Jackson, M. G. Kane, I. G. Hill, M. S. Hammond, J. Campi, B. K. Greening, J. Francl, and J. West, Appl. Phys. Lett. **80**, 1088 (2002).
[3] H. Klauk, D. J. Gundlach, and T. N. Jackson, IEEE Trans. Electron Devices **20**, 289 (1999).
[4] J. A. Rogers, Z. Bao, and V. R. Raju, Appl. Phys. Lett. **72**, 2716 (1998).
[5] J. A. Rogers, Z. Bao, A. Makhija, P. Braun, Adv. Mater. (Weinheim, Ger.) **11**, 741 (1999).
[6] H. Sirringhaus, T. Kawase, R. H. Friend, T. Shimoda, M. Inbasekaran, W. Wu, and E. P. Woo, Science **290**, 2123 (2000).
[7] K. Cheng, M. Yang, W. Chiu, C. Huang, J. Chang, T. Ying, and Y. Yang, Macromol. Rapid Commun. **26**(4), 247 (2005).
[8] L. Burgi, T. J. Richards, R. H. Friend, and H. Sirringhaus, Appl. Phys. Lett. **94**, 6129 (2003).
[9] C. W. Chu, S. H. Li, C. W. Chen, V. Shrotriya, and Y. Yang, Appl. Phys. Lett. **87**, 193508 (2005).